LANGMUIR

Biological and Environmental Phenomena at the Interface

Three-dimensional Bacterial Motions Near a Surface Investigated by Digital Holographic Microscopy: Effect of Surface Stiffness

Qingmei Peng, Xin Zhou, Zhi Wang, Qingyi Xie, Chunfeng Ma, Guangzhao Zhang, and Xiangjun Gong

Langmuir, **Just Accepted Manuscript** • DOI: 10.1021/acs.langmuir.9b02103 • Publication Date (Web): 18 Aug 2019

Three-dimensional Bacterial Motions Near a Surface Investigated by Digital Holographic Microscopy: Effect of Surface Stiffness

Qingmei Peng, Xin Zhou, Zhi Wang, Qingyi Xie, Chunfeng Ma, Guangzhao Zhang, Xiangjun Gong*

Faculty of Materials Science and Engineering, South China University of Technology, Guangzhou 510640, P. R. China

*Correspondence should be addressed to X.G. (*E-mail*: msxjgong@scut.edu.cn).

Abstract

Surface stiffness plays a critical role in bacterial adhesion but the mechanism is unclear since the bacterial motion before adhesion is overlooked. Herein, the three-dimensional (3D) motions of *Escherichia coli* (*E. coli*) and *Pseudonomas*. sp nov 776 onto poly(dimethylsiloxane) (PDMS) surfaces with varying stiffness before adhering were monitored by digital holographic microscopy (DHM). As the Young's modulus (E) of PDMS surface decreases from 278.1 to 3.4 MPa, the adhered *E. coli* and *Pseudonomas*. sp decrease in number by 40.4 and 34.9 % respectively. Atomic force microscopy (AFM) measurements show that the adhesion force of bacteria to the surface declines with the decreased surface stiffness. In contrast, a non-tumbling mutant of adhered *E. coli* (HCB1414 with adaptive function being partially deficient) decreases much less (by 18.4 %). On the other hand, the tumble frequency (F_t) of *E. coli* HCB1 and flick frequency (F_f) of *Pseudomonas* sp. increase as the surface stiffness decreases, and the motion bias (B_θ) of *Pseudomonas* sp. also increases. These facts clearly indicate that the bacteria have adapted responses to the surface stiffness.

RNA-sequencing (RNA-seq) reveals that the downregulated Cph2 and CsrA as well as the upregulated GcvA of swimming *E. coli* HCB1 in bulk near the softer surface promote the bacterial motility.

Keywords: *surface stiffness, digital holographic microscopy, bacterial adhesion, bacterial tracking, RNA-sequencing*

Introduction

Bacterial adhesion is the primary step of biofilm formation, which is usually the start of marine biofouling,[1,2] medical infection,[3] and food contamination.[4,5] It is recognized that physicochemical properties of the surface, *i.e.*, surface hydrophobicity,[6] charges,[7] topography[8,9] and stiffness[10,11] regulate bacterial adhesion. The effects of surface stiffness on bacterial adhesion have drawn attentions in the past years. It was reported that the adhesion of *S. epidermidis* was positively correlated with the surface stiffness with E of 0.8 to 80 MPa by using polyelectrolyte multiplayer thin films as a model.[12] For poly(ethylene glycol) dimethacrylate (PEGDMA) and agar hydrogel surface, less *E. coli* and *S. aureus* adhere onto the softer surface (E rangs from 44 kPa to 6.5 MPa).[13] *Pseudoalteromonas* sp. D41, a marine strain, also showed stronger adhesion to rigid surfaces,[14] which was explained by the so-called adapted response of bacteria in a proteic study. In contrast, *E. coli* and *P. aeruginosa* exhibited weaker adhesion as

the PDMS surface stiffness increases.[11] Likewise, *Acanthamoeba castellanii* (*A.castellanii*), a eukaryotic protist, had an increased cell adhesion number with the decreasing *E* of PDMS substrate.[15]

The surface stiffness also affects bacterial motions during adhesion and biofilm growth. A two-dimensional cell tracking technique was utilized to observe the movement of *E. coli* attached on PDMS surfaces with *E* at 0.1 to 2.6 MPa.[10] It revealed the flagellar motor of *E. coli* involves in an active response to surface stiffness. Such adaptive behavior was also observed in *P. aeruginosa*.[16] The cells slingshot more on softer poly(*N*-isopropylacrylamide) (PNIPAM) surfaces at a shear-thinning condition, which facilitates their surface crawling. The growth rate of *E. coli* and *P. aeruginosa* biofilms, as well as the size and antibiotic susceptibility on PDMS increase as the surface stiffness decreases.[11] The growth of *E. coli* colonies is faster on a film with E = 30 kPa than the one with E = 150 kPa.[17] Although many efforts have been made to correlate bacterial adhesion to surface stiffness, little attention was paid to how bacteria regulate their motions in response to the surface stiffness before adhesion.[18,19]

Attributed to the fact that the stiffness of the PDMS films prepared by spin coating is thickness dependent due to different shear stress during fabrication[20], we engineered PDMS surfaces with varying stiffness by tuning their thickness on glass coveslips. In this manner, the surface chemistry and topography change slightly and the bacterial responses to the surface stiffness can be solely examined. A home-made

digital holographic microscopy (DHM) is utilized to track the planktonic bacteria (*E. coli* and a marine bacteria *Pseudomonas* sp.) before adhesion in 3D with time and spatial dependence. It has been applied to monitor the 3D dynamics of bacteria upon polymeric surfaces with different hydrophobicity[6] and degradation rates.[21] The adhesion forces between bacteria and surfaces were assessed by atomic force microscopy (AFM). Moreover, RNA sequencing (RNA-seq) of bacteria was applied for illuminating the mechanisms at a molecular level.

Experimental Section

Surface preparation. PDMS surface was prepared by SYLGARD184 Silicone Elastomer Kit (Dow Corning). The ratio (w/w) of the prepolymer to curing agent was fixed at 10:1. The concentration of PDMS to tetrahydrofuran (THF, Sinopharm) were 5, 15 and 25 % (w/v). The coverslips (22×22 mm, Fisher Scientific) were cleaned by immersion in a fresh piranha solution (H_2O_2/H_2SO_4, 3:7 v/v; 90 ºC) for 2 h, then sonication in deionized water (DI water) and ethanol for 5 min, respectively, and dried with nitrogen before use.

PDMS films with thickness of 0.4, 0.8, and 2.0 μm (Figure S1) were prepared on the cleaned coverslips by spin-coating 200 μL of 5, 15 and 25 % PDMS/THF solutions through a spin-coater (KW-4, CHEMAT) at 3,000 rpm in air, respectively. The coated coverslips were cured at 80 °C for 2 h, and incubated at room temperature

for 24 h to be fully cross-linked. The cured surfaces were sterilized by washing with ethanol and dried with nitrogen gas.

Surface characterization. AFM (XE-100, Park Systems) was utilized to measure the thickness of the PDMS coatings. The measurement was conducted with rectangular silicon cantilever (NCHR, spring constant 42 N/m, Nanosensors) in a tapping mode. The PDMS surfaces were scraped with a blade to expose the substrate, the probe was then allowed to slowly approach and scan imaging. With the relative height between the PDMS film and substrate in the surface topography, the thickness of the coatings was obtained.[22]

Young's modulus (E) determined by force-distance curves executed with AFM was used to quantify the stiffness of the surface.[6] The recorded force-indentation curves were fit to the Hertzian contact model at the linear elasticity region (Figure S2). E of the surfaces was obtained by the following equation:[23]

$$F = \frac{E}{1-\upsilon^2}\frac{\tan\alpha}{\sqrt{2}}\delta^2 \quad (1)$$

where υ is the Poisson's ratio of PDMS surface which is assumed to be 0.5.[24] α is the four-sided pyramidalface angle of cantilever tip (22°). The indentation depth $\delta = d_p - d_f$, in which d_p is the piezo displacement of AFM, and d_f is the deflection of the cantilever free end. F is the applied force obtained from the force curve.

Surface roughness (R_q) was measured with rectangular silicon cantilever in the

tapping mode. All AFM measurements were conducted in air at 25 °C with at least three times on different positions. Surface potential (ζ) was acquired in 10 mM NaCl solution by using a DelsaNano C particle and zeta Potential Analyzer (Beckman Coulter). Theta optical tensiometer (T200-Auto1B, Biolin Scientific) was performed to obtain the static water contact angle (WCA) of these surfaces. The elemental composition was analyzed by X-ray photoelectron spectrometer (Axis uHru DCD, Krates, see Figure S3). Surface characterization methods mentioned above were repeated for three times.

Bacterial strain and culture. A wild-type *Escherichia coli* (HCB1), a smooth-swimming mutant (HCB1414 *ΔcheY ΔcheZ*, non-tumbling motion), and a marine bacteria *Pseudomonas* sp. nov 776 isolated from marine subtidal biofilms were used in this study. *E. coli* and *Pseudomonas* sp. cells were streaked on luria broth (LB) and marine agar (MA) plates, respectively. A monoclonal colony was inoculated into a fresh growth medium. After growing up to mid-log phase (OD_{600} = 0.4), the bacterial suspension was diluted into a motility buffer (MB) with the ratio of 1:10 (v/v), more details were described elsewhere.[21]

Before DHM observation, the suspension was injected into a chamber (16 mm of length, 1 mm of width, 100 μm of height) consisting of a PDMS microfluidic chip (Suzhou Wenhao Microfluidic Tech. Co., Ltd., China) and a PDMS coated coverslip. The chip was treated in a plasma cleaner (PDC-002, Harrick Plasma) for 10 min before sticking to the coated substrates. Motility buffer was continuously injected into

the channel for 15 min before observation. Since the experiment was conducted under a static condition, the chip would be sealed after the channel was filled with the suspension.

Measurements of bacterial adhesion force. AFM was performed to measure the adhesion force between a colloidal probe covered with bacteria and the surface. A 23 μm diameter SiO_2 microsphere (Suzhou Nano-Micro Technology Co., Ltd, China) was attached to the silicon nitride tip on the end of the cantilever to make a colloidal probe. The colloidal probe was treated with plasma for 10 min and disposed in a 1% (w/v) poly(ethyleneimine) (PEI, M_w = 1800, Aladdin) for 2.5 h, then cleaned with DI water. The treatment of PEI enabled the bacteria to be firmly adhered on SiO_2 microsphere. Bacteria were prepared by centrifugating (2000 g, 5 min) the mid-exponential phase bacterial suspension for three times, dispersed into a 3% (w/v) glutaraldehyde solution at 4 ºC for 2.5 h, and cleaned with MB for two times.[6,25] 10 μL of the treated bacterial suspension was added onto a cleaned silicon wafer. Afterwards, the colloidal probe was brought proximity to the drop and immersed in it for 15 min to enhance the coverage of bacteria. The interactions between bacteria and the surface in MB were measured immediately. The surface force separation curves were obtained under a contact mode. The adhesion force corresponds to the maximum tip deflection upon the retraction of the cantilever.[26] Each attraction force (γ) obtained from the force statistics was measured at least three times (12 different positions).

Digital holographic microscopy (DHM). DHM for 3D bacterial tracking is based on

an in-line configuration integrated with an inverted microscope (IX-83, Olympus, Japan).[27,28] A 40× microscope objective (NA = 0.6, LUCPLFLN40×, Olympus) was utilized. The bacterial suspension was illuminated uniformly by a collimated light-emitting diode (LED, λ = 455 nm, Thorlabs, US), and part of the incident light was scattered by the suspension. Real-time holograms of 1024 × 1024 pixels formed by the interference of the scattered and unscattered incident light were recorded using a sCMOS camera (Zyla-5.5-CL3, 6.5 μm/pixel, Andor Technology, UK) at 20 frames/s. More details were introduced elsewhere.[6,21] DHM experiments for each surface with the specific stiffness were repeated for four times and performed at 25 °C. Each hologram would be subtracted by a background image which was generated by averaging all images recorded in 2 min to aviod the stationary noise. Bacterial adhesion is quantified as the number of bacteira adhered onto the background image (N_b). The independent 3D coordinates of each bacterium was based on Rayleigh-Sommerfeld proporgation[27,29] and further connected to continuous trajectories by a home-made programme. The bottom surface (z = 0) was set as the location of bacteria with the shortest reconstructed distance to the focal plane, then a relative height (z) of bacteria in different positions could be obtained.

Data Processing. Mean square displacement (*MSD*) was used to describe the motility of bacteria.[21] The *MSD* - Δt curve was fit by the equation $MSD(\Delta t) = D(\Delta t)^{v}$, and the index v was obtained from the first 10 % continuous points of each *MSD* - Δt curve. The motion of the observed bacteria was classified into active and subdiffusive by the

power index υ. $\upsilon \geq 1$ represents an active motion, while $\upsilon < 1$ corresponds to a subdiffusive motion. N_{sub} refers to the number of subdiffusive motion of bacteria upon surfaces ($0 < z < 10$ μm).

3D orientation, motion patterns, density distribution $n(z)$, and collision analysis were all derived from the 3D trajectories of the bacteria with the active motion. The bacterial orientation was defined as the angle (θ) between the surface normal and swimming direction of bacteria. When $\theta > 90°$ (θ_{down}), the bacteria swim toward the surface but away from the surface at $\theta < 90°$ (θ_{up}). *E. coli* HCB1 cells swim by rotating a bundle of flagella as the flagellar motors turn in a counterclockwise direction.[30] A tumble defined as an obvious change in the direction (over 75 degree) of trajectory is caused by the dispersal of the flagellar bundle or clockwise rotation of the motors.[31] *Pseudomonas* sp. swimming by rotating a single polar fagellum, moves in a three-step swimming pattern containing forward, reverse and flick.[30,32] The flagellum will flick and choose a new direction randomly.[33] The critical angles of the flick and reverse event are 70 and 110 degree in our analysis. Tumble frequency (F_t) and flick frequency (F_f) were applied to describe the tumble and flick occurrence of bacteria per second. Besides, the distance range from the surface where 50 % bacteria cells locate in was described as D_r. An increased D_r indicates a dispersed distribution. All results were compared using a Student's *t* test (between the cases of surface with E = 278.1 MPa and the other softer surfaces, respectively) or one-way ANOVA. Significance was assumed when $p < 0.05$.

RNA sequencing (RNA-seq). *E. coli* HCB1 was used for RNA extraction. *E. coli* was collected from the suspensions upon surfaces with E = 278.1 (S_{stiff}) and 3.4 MPa (S_{soft}), respectively, and with an independent replicate. The samples were then centrifugated at 4 ^{o}C, 8000 rpm for 5 min. Removed the supernatant and stored at -80 ^{o}C. Trizol method was performed to extract the total RNA of each sample. RNA quality was detected by agarose gel electrophoresis. Agilent 2100 and Agilent 2100 RNA 6000 Pico kit were applied to identify the purity and concentration of the RNA-seq sequencing samples. Oligotex mRNA Kits Midi were utilized to enrich the mRNA. The small RNA libraries were sequenced on the Illumina sequencing platform by Genedenovo Biotechnology Co., Ltd (Guangzhou, China). The sequencing depth of samples was 1 G. After the sequencing run, paired-end nucleotide reads were further filtered to obtain high quality clean reads and mapped to the reference genomic sequence of *E. coli* K-12 MG1655 (NCBI: txid511145).[34] The unique mapped ratios of samples to reference genes are distributed between 93.85 to 95.64%. The reproducibility of the two replicates could be reflected by the Pearson correlation shown in Figure S4. The coefficients of S_{stiff} and S_{soft} are 0.98 and 0.87, respectively, indicating a relatively good biological repeatability. The filter was set as $p < 0.05$, fold change (FC) >1.5 to analyze the differential expression of genes.

Results and Discussion

PDMS is a viscoelastic material. Figure S5 implies the dynamic stiffness (k_d) and the loss modulus (G''), which indicate the surface viscoelasticity correlated negatively with the thickness of the PDMS films. For better comparison with previous works, the Young's modulus (E) was used to describe the stiffness of the PDMS surfaces. Accordingly, for PDMS coatings with thickness of 0.4, 0.8, and 2 μm, E inversely related to the thickness are 278.1 ± 147.6, 35.0 ± 13.0, and 3.4 ± 0.4 MPa, respectively (Figure 1a). E of the substrate (glass coverslip) is dozens to hundreds GPa,[35] which is much higher than that of PDMS. As a result, the increased modulus for a reduced thickness (less than 2 μm) is understandable because the influence from the substrate becomes significant. However, the thickness does not make difference in surface roughness (R_q), surface potential (ξ) and static water contact angle (CA) between the surfaces (Figure 1b, 1c and 1d). The surface can be treated as uncharged since they have a potential of ± 10 mV,[36,37] and the effect of electrostatic force can be neglected. The surface composition analysis in Figure S3 further indicates the little distinction of elemental mass concentration between surfaces. Thus, surfaces with varying stiffness and consistent surface chemistry were obtained by tuning the film thickness.

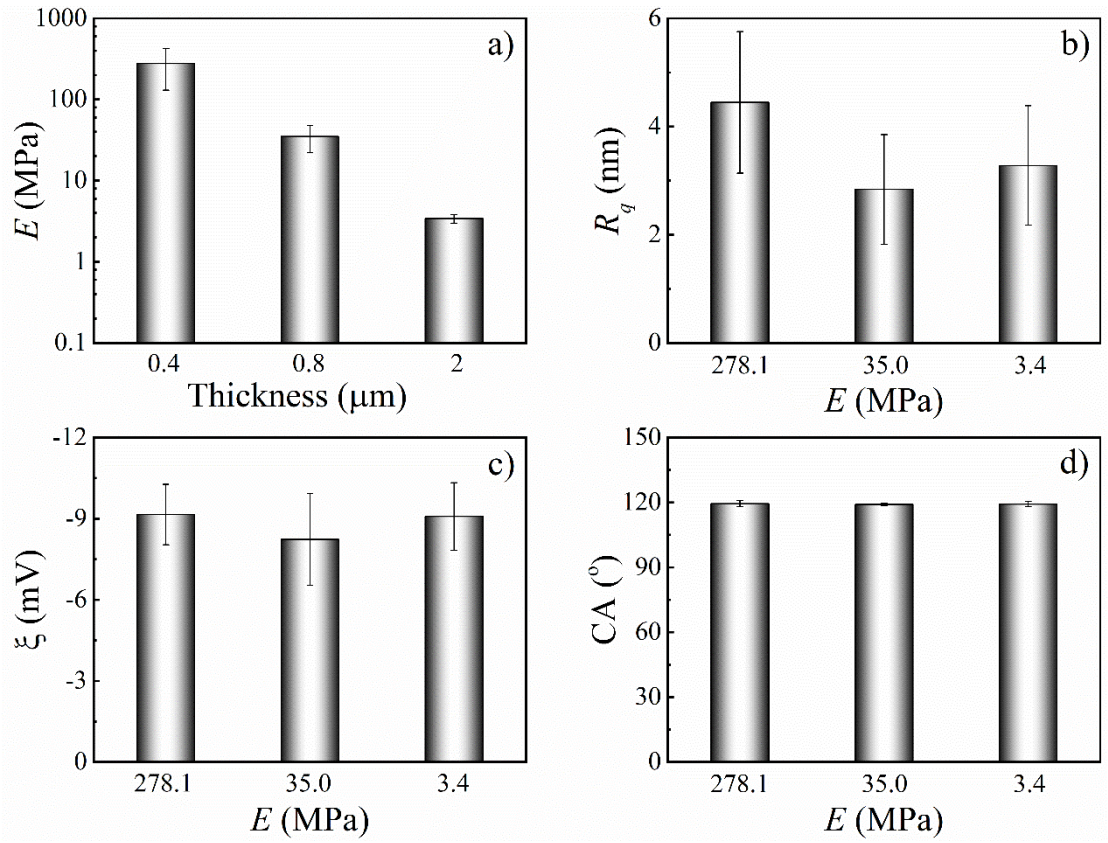

Figure 1. Characterization of PDMS coatings. (a) Young's modulus (*E*) of the coatings as a funtion of thickness. (b) Surface roughness (R_q). (c) Surface potential (ξ). (d) Water contact angle (CA).

Surface adhesion of *E. coli* HCB1 and *Pseudomonas* sp. was assessed (Figure 2a). For HCB1, compared with the adhered bacteria ($N_b = 1.77\times10^5 \cdot cm^{-2}$) on a glass surface, N_b obviously decreases for all the PDMS surfaces which is softer. Similarly, Figure 2a showed N_b decreases by 40.4 and 34.9 % for *E. coli* HCB1 and *Pseudomonas* sp. as the Young's modulus decreases from 278.1 to 3.4 MPa, indicating the bacteria prefer to adhere onto the stiffer surface. Similar phenomena

were observed for *E. coli* and *S. aureus* on the surfaces of synthetic polymer and biopolymer hydrogels,[13] where the stiffness was regulated by the component concentration. Bacteria tend to exhibit subdiffusive motion before irreversible adhesion, which is mediated by the flagella or pili.[38,39] Therefore, N_{sub}, defined as the number of bacteria presenting a subdiffusive motion near the surface ($0 < z < 10$ μm) was calculated. As shown in Figure 2b, N_{sub} of *E. coli* HCB1 and *Pseudomonas* sp. significantly decreases as the surface stiffness decreases ($p < 0.05$, one-way ANOVA). This agrees with the reduced N_b for the softer surface in Figure 2a.

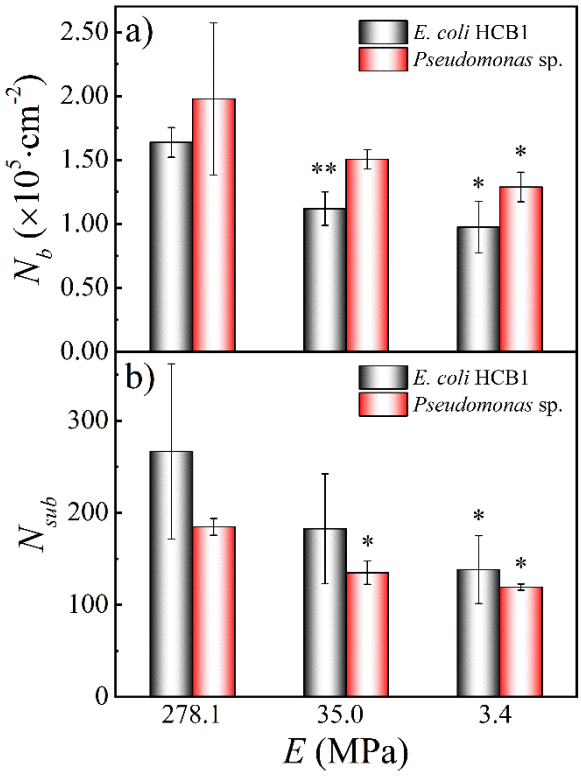

Figure 2. (a) Adhesion number (N_b) and (b) subdiffusive ($\upsilon < 1$) population density (N_{sub}) ($0 < z < 10$ μm) of *E. coli* HCB1 and *Pseudomonas* sp. upon PDMS surfaces with varying stiffness. (*) and (**) denotes significant difference at $p < 0.05$ and 0.01, compared to the results for the surface

with E = 278.1 MPa and determined by t test.

The reduced N_b can be explained by adhesion force (γ) between bacteria and surface measured by AFM (Figure 3). As the Young's modulus decreases from 278.1 to 3.4 MPa, γ for *E. coli* HCB1 significantly decreases from ~ 800 to ~ 170 nN while γ for *Pseudomonas* sp. decreases from ~ 2200 to ~ 300 nN. It might be the consequence of the decreased viscosity as the surface becomes softer (shown in Figure S5b). Accordingly, when bacteria collide with the surface with a force of 2.1 pN,[6] the surface with E = 3.4 MPa has a deformation of 0.62 nm^2, much more than that 7.6×10^{-3} nm^2 of the surface with E = 278.1 MPa. The softer surface with larger deformation is more difficult for bacteria to land and adhere on, which leads to a reduced adhesion force, and thus significantly decreasing N_b.

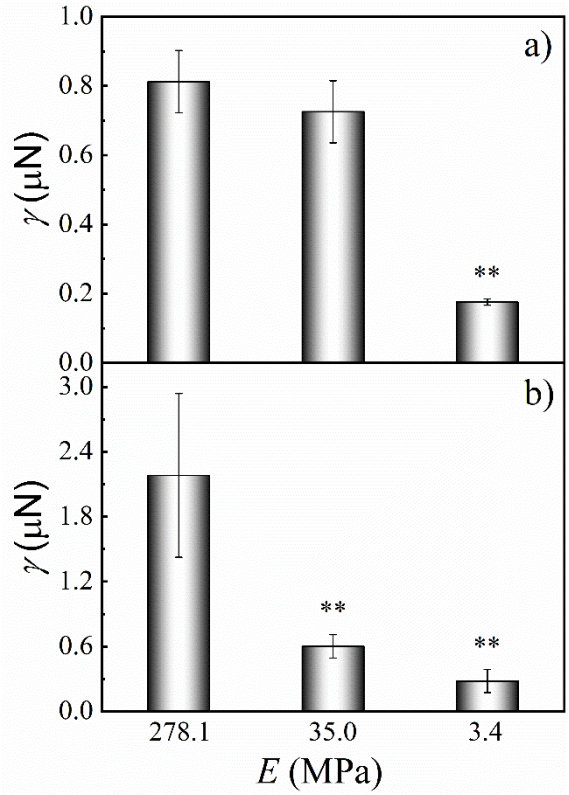

Figure 3. Adhesion force (γ) between (a) *E. coli* HCB1, (b) *Pseudomonas* sp. and PDMS surfaces with varying stiffness. (**) denotes significant difference at $p < 0.01$, compared to the results for the surface with $E = 278.1$ MPa and determined by *t* test.

We also examined the 3D orientation (θ) of actively swimming bacteria. The motion bias (B_θ) defined as the ratio of θ_{up} to θ_{down} was used to describe the motion tendency of bacteria. $B_\theta = 1$ represents the uniformly orientation of bacteria, while $B_\theta > 1$ and < 1 indicates bacteria tend to move away from the surface and accumulate on the surface. Figure 4a shows B_θ of *E. coli* HCB1 makes small difference ($p = 0.09$, one-way ANOVA) among the surfaces with varying stiffness. In contrast, B_θ of

Pseudomonas sp. increases from 0.95 to 1.1 as the surface becomes softer. The facts indicate *Pseudomonas* sp. cells tend to swim away from the surface with E = 3.4 MPa but accumulate on the surface with E = 278.1 MPa. This is in accordance with the density distribution (heatmaps) of *Pseudomonas* sp. shown in Figure 4b and 4c, where the bacteria in $0 < z < 5$ μm upon surface with E = 278.1 MPa is much denser than the 3.4 MPa one.

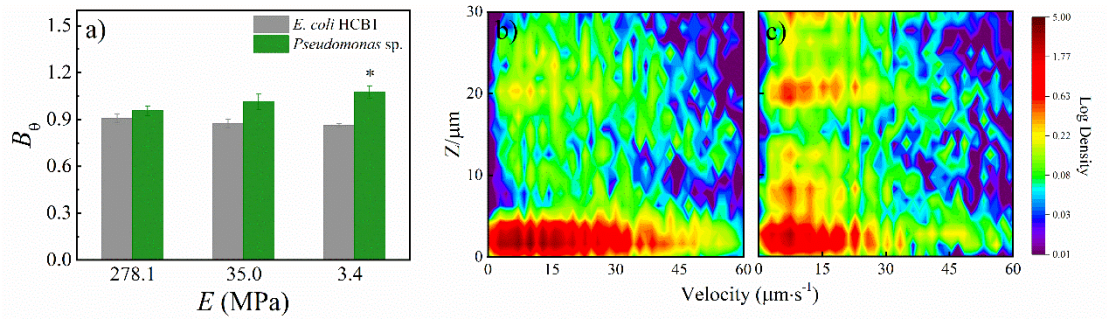

Figure 4. Orientation of bacteria upon PDMS surfaces with different stiffness. (a) Motion bias (B_θ) of actively swimming *E.coli* HCB1 and *Pseudomonas* sp. upon PDMS surfaces. ($B_\theta = \theta_{up}/\theta_{down}$, active bacteria in the range of 0 to 5 μm). Density distribution (heatmaps) of instantaneous 3D velocities and distances (z = 0 to 30 μm) from the (b) 278.1 and (c) 3.4 MPa surfaces for *Pseudomonas* sp. Color bars represent the relative density of data points with a logarithmic scale. (*) denotes significant difference at $p < 0.05$, compared to the results for the surface with E = 278.1 MPa group and determined by t test.

Figure 5a and 5b show the typical swimming trajectories of *E. coli* HCB1 and *Pseudomonas* sp, respectively. Unlike the molecules or polymers undergo diffusion or

subdiffusion determined by the hydrodynamic interactions near a surface,[40] bacteria swim actively and present many unique motion features. The swimming pattern of the peritrichous bacteria like *E. coli* HCB1 is divided into linear forward swimming (run) and abrupt changes in direction (tumble), which is highly associated with the chemotactic behavior of bacteria.[41] F_t of *E. coli* HCB1 increases from 1.21 to 1.49 when the Young's modulus decreases from 278.1 to 3.4 MPa (Figure 5c), and it is significantly larger than F_t of HCB1 upon the glass surface reported in our former work.[6] The polarly uni-flagellated marine bacteria *Pseudomonas* sp. execute a cyclic swimming pattern (forward, reverse, and flick). It is known that flick event is related to tactical behaviors of bacteria in response to the environment.[32,33] As shown in Figure 5d, F_f is significantly raised from 1.06 to 1.44. This tendency agrees with the similiar bacterial orientation of *Pseudomonas* sp. near different surfaces (Figure 4a). Therefore, the increase of the tumble and flick events are related to the adapted response of bacteria to the surfaces with different stiffness. We will come back to this later.

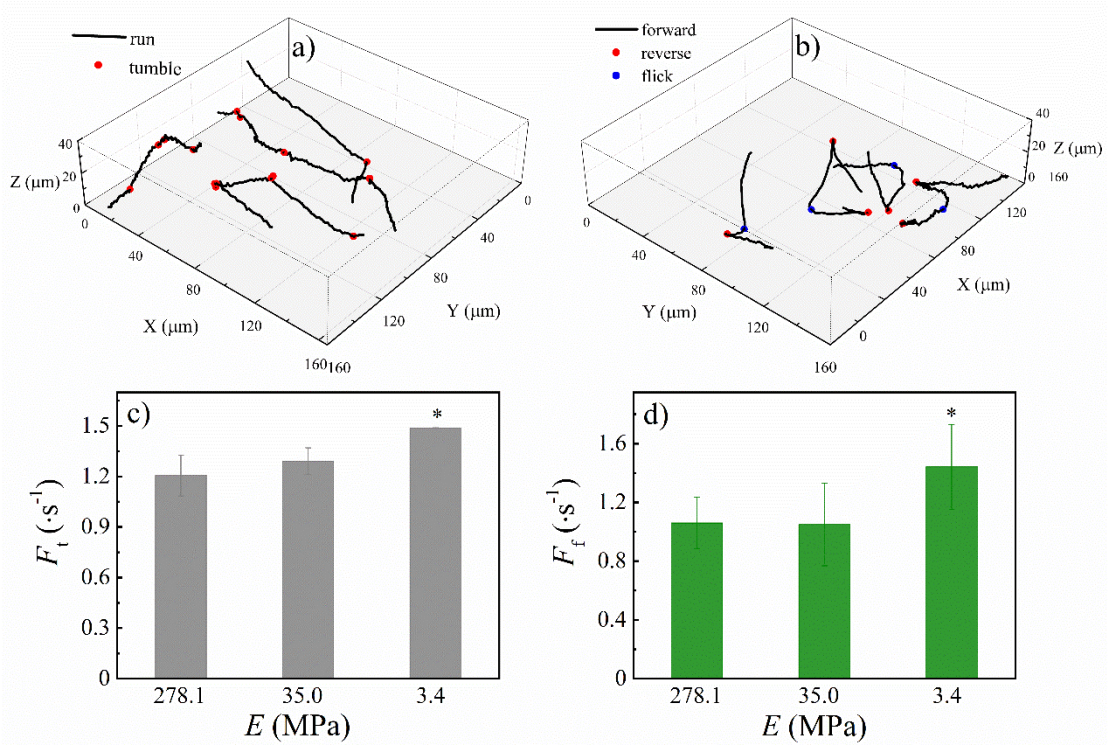

Figure 5. Typical trajectories of (a) *E. coli* HCB1 and (b) *Pseudomonas* sp. Tumble frequency (F_t) and flick frequency (F_f) of (c) *E. coli* HCB1 and (d) *Pseudomonas* sp., respectively. (*) denotes significant difference at $p < 0.05$, compared to the results for the surface with E = 278.1 MPa group and determined by *t* test.

As discussed above, the decreased N_b of bacteria upon the softer surface results from interactions between bacteria and surface with varying stiffness, *i.e.*, adhesion force, and adapted responses of bacteria to the surroundings with different stiffness, *i.e.*, tumble or flick. Thus, the adhesion of a chemotaxis deficient mutant of *E. coli*, *i.e.*, non-tumbling HCB1414 was examined to evaluate their contribution. Figure S6 and S7 show that N_b decreases by 18.4 % as the Young's modulus decreases from

278.1 to 3.4 MPa. Since HCB1414 does not exhibit the typical adapted response (tumble), the reduction in N_b should be mainly attributed to the weaker bacteria-surface interactions as surface stiffness decreases. With HCB1414 as the reference, the contribution from the bacteria-surface interactions for HCB1 is estimated to be 45.5 %.

The typical density distributions of HCB1414 and HCB1 actively swimming near the surface with E = 278.1 MPa are shown in Figure 6a. Bacteria swim and accumulate in the vicinity of surfaces before adhesion because of the hydrodynamic interaction.[42,43] HCB1414 without the motion of tumble tends to be more concentrated upon surfaces. This is consistent with the result that the total $n(z)$ at near-surface region ($0 < z < 3$ μm) of HCB1414 is about 0.5, obviously larger than that of HCB1 (0.2), indicating that the near-surface density distribution increases as *E. coli* lacking the adapted response (tumble). Meanwhile, as shown in Figure 6b, D_r of HCB1414 slightly increases from 2.87 to 4.89 μm, arising from hydrodynamic interactions upon the surfaces with E = 278.1 to 3.4 MPa. For HCB1, D_r increases from 14.22 to 19.22 μm, in which bacteria-surface interactions contributes by 40.4 % obtained from the increment of D_r for HCB1414 to that for HCB1, and the adapted responses by 59.6 %. Generally, they are consistent with the results about N_b.

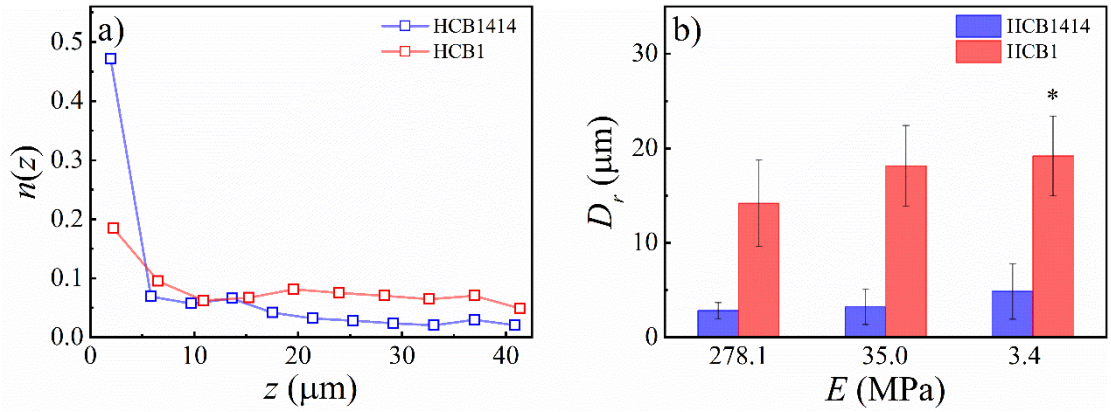

Figure 6. (a) Density distribution ($n(z)$) of bacteria upon the PDMS surface (E = 278.1 MPa). (b) The distribution range (D_r) of 0 - 50 % HCB1414 and HCB1 cells closer to the surface. (*) denotes significant difference at $p < 0.05$, compared to the results for the surface with E = 278.1 MPa group and determined by t test.

Finally, RNA-seq was employed to explore the molecular-level mechanism of bacterial behaviors upon surfaces with different stiffness. We collected *E. coli* HCB1 in bulk instead of the attached cells uopn surfaces with E = 278.1 (S_{stiff}) and 3.4 MPa (S_{soft}) to confirm the adapted responses of swimming bacteria to surface stiffness. There are 189 differential expression genes, 82 upregulated and 107 downregulated (Figure S8). Note that a GGDEF domain-containing protein Cph2 which can indirect regulate the level of the second messenger cyclic dimeric guanosine monophosphate (c-di-GMP)[44] is downregulation in S_{soft} compared to S_{stiff} (Figure 7a). C-di-GMP plays an important role in sensing environmental cues.[45,46] The model of c-di-GMP molecular regulation module is shown in Figure S9. The increased level of

intracellular c-di-GMP will inhibit the bacterial motility and promote biofilm formation.[47] Meanwhile, the c-di-GMP level is connected with the surface stiffness.[48] Figure S10 shows the 3D velocity (V_{3D}) increment of bacteria from z = 10 to 1 μm. The increment changes from -0.14 to 17.04 %, -1.88 to 7.59 % of *E. coli* HCB1 and *Pseudomonas* sp. upon the surfaces with E = 278.1 to 3.4 MPa. Clearly, a higher motility of bacteria is observed when surface becomes softer, which is in accordance with the phenomenon in Figure 5. As a result, the decrease of the GGDEF domain protein reduces the intracellular c-di-GMP level but improves the motility of bacteria and thus decreases N_b on the softer surface.

Besides, in the process of KEGG pathway enrichment, downregulated CsrA and upregulated GcvA of S_{soft} in the pathway of biofilm formation is correlated to bacterial adhesion (Figure 7a). As shown in Figure 7b, the decrease of CsrA could lower the biosynthesis of glycogen and poly(*N*-acetyl-glucosamine) (PGA), which is related to exopolysaccharides (EPS). The adhesion of bacteria to a surface can be enhanced by EPS.[49,50] EPS produced by bacteria reduces as the surface becomes softer. This can account for the decreased adhesion force in Figure 3. Meanwhile, the upregulated GcvA shows an indirect effect on the inhibition of biofilm formation, thus decreasing N_b on the softer surface.

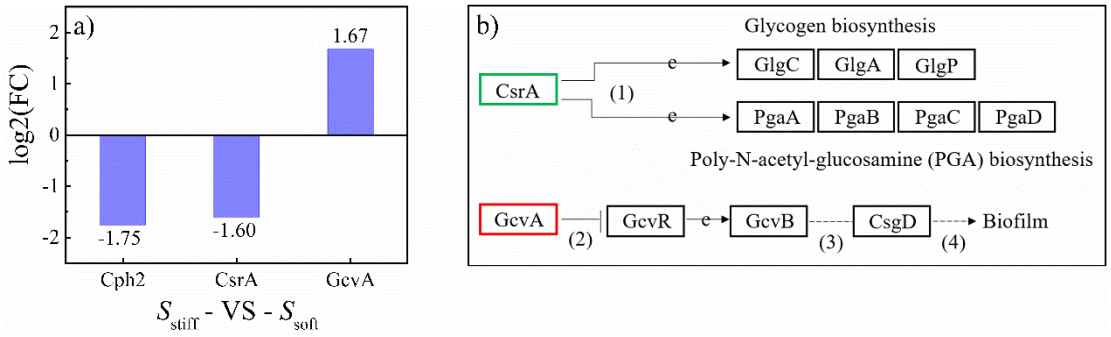

Figure 7. (a) The difference of Cph2, CsrA, and GcvA expression level in S_{soft} compared to S_{stiff}. FC refers to fold change. (b) Partial pathway for biofilm formation. (1) expression (2) inhibition (3) change of state (4) indirect effect. (Green and red boxes mean downregulated and upregulated genes, respectively.)

Conclusion

The 3D motions of *E. coli* and *Pseudomonas* sp. upon PDMS surfaces with different stiffness were tracked by DHM. For *E. coli* wild strain HCB1 and marine bacteria *Pseudonomas* sp., the adhering and subdiffusively swimming populations significantly decrease as the surface becomes softer. Adhesion number of a non-tumbling *E. coli* HCB1414 which is a mutant with adaptive function partially deficient decreases much less upon the softer surface than the above two strains. AFM measurements indicate the reduction of the adhesion force of bacteria to the surface as the surface stiffness decreases. From DHM measurements, adaptive behaviors, *i.e.*, tumble motions for HCB1 and flick motions for *Pseudomonas* sp. become more frequent as the surface stiffness decreases, while the motion bias (B_θ) of *Pseudomonas*

sp. increases. RNA-seq of HCB1 reveals that the downregulation of Cph2 enhances the bacterial motility, while the downregulation of CsrA and upregulation of GcvA inhibit the bacterial adhesion. These results imply surface stiffness modulates bacterial adhesion through physical interaction (40%) and bacterial adaptive responses (60%).

ASSOCIATED CONTENT

Supporting Information

Thickness of PDMS coatings; Fitting process of Young's modulus by Hertzian model; XPS scan spectra and elemental mass concentration; Correlation Heatmap; k_d and G'' of the PDMS surface; N_b of *E. coli* HCB1414; P_d of bacteria; Statistics of differential expression genes; A model of c-di-GMP molecular regulation module; Variable of V_{3D} from z = 10 to 1μm.

AUTHOR INFORMATION

Corresponding Authors

*Email: msxjgong@scut.edu.cn.

Notes

The authors declare no competing financial interests.

ACKNOWLEDGEMENTS

The financial support of National Natural Science Foundation of China (21574046, 51573061), the National Natural Science Foundation of Guangdong Province (2019B030301003) and the Fundamental Research Funds for the Central Universities is acknowledged.

REFERENCES

(1) Priyanka, P.; Arun, A. B.; Young, C. C.; Rekha, P. D. Prospecting exopolysaccharides produced by selected bacteria associated with marine organisms for biotechnological applications. *Chinese J. Polym. Sci.* **2015**, *33* (2), 236-244.

(2) Cooksey, K. E.; Wigglesworth-Cooksey, B. Adhesion of bacteria and diatoms to surfaces in the sea: a review. *Aquat. Microb. Ecol.* **1995**, *9*, 87−96.

(3) Haussler, S.; Parsek, M. R. Biofilms 2009: New Perspectives at the Heart of Surface-Associated Microbial Communities. *J. Bacteriol.* **2010**, *192* (12), 2941-2949.

(4) Costerton, J. W.; Stewart, P. S.; Greenberg, E. P. Bacterial biofilms: A common cause of persistent infections. *Science* **1999**, *284* (5418), 1318-1322.

(5) Miao, J.; Liang, Y. R.; Chen, L. Q.; Wang, W. X.; Wang, J. W.; Li, B.; Li, L.; Chen, D. Q.; Xu, Z. B. Formation and development of Staphylococcus biofilm: With

focus on food safety. *J. Food Saf.* **2017**, *37* (4), 11.

(6) Qi, M.; Gong, X.; Wu, B.; Zhang, G. Landing Dynamics of Swimming Bacteria on a Polymeric Surface: Effect of Surface Properties. *Langmuir* **2017**, *33* (14), 3525-3533.

(7) Campoccia, D.; Montanaro, L.; Arciola, C. R. A review of the biomaterials technologies for infection-resistant surfaces. *Biomaterials* **2013**, *34* (34), 8533-8554.

(8) Hsu, L. C.; Fang, J.; Borca-Tasciuc, D. A.; Worobo, R. W.; Moraru, C. I. Effect of Micro- and Nanoscale Topography on the Adhesion of Bacterial Cells to Solid Surfaces. *Applied and environmental microbiology* **2013**, *79* (8), 2703-2712.

(9) Diaz, C.; Schilardi, P. L.; Salvarezza, R. C.; Fernandez Lorenzo de Mele, M. Have flagella a preferred orientation during early stages of biofilm formation?: AFM study using patterned substrates. *Colloids and Surfaces B-Biointerfaces* **2011**, *82* (2), 536-542.

(10) Song, F.; Brasch, M. E.; Wang, H.; Henderson, J. H.; Sauer, K.; Ren, D. How Bacteria Respond to Material Stiffness during Attachment: A Role of Escherichia coli Flagellar Motility. *ACS Appl. Mater. Inter.* **2017**, *9* (27), 22176-22184.

(11) Song, F.; Ren, D. Stiffness of cross-linked poly(dimethylsiloxane) affects bacterial adhesion and antibiotic susceptibility of attached cells. *Langmuir* **2014**, *30* (34), 10354-10362.

(12) Lichter, J. A.; Thompson, M. T.; Delgadillo, M.; Nishikawa, T.; Rubner, M. F.; Vliet, K. J. V. Substrata Mechanical Stiffness Can Regulate Adhesion of Viable Bacteria. *Biomacromolecules* **2008**, *9* (6), 1571–1578.

(13) Kolewe, K. W.; Peyton, S. R.; Schiffman, J. D. Fewer Bacteria Adhere to Softer Hydrogels. *ACS Appl. Mater. Inter.* **2015**, *7* (35), 19562-19569.

(14) Guegan, C.; Garderes, J.; Le Pennec, G.; Gaillard, F.; Fay, F.; Linossier, I.; Herry, J. M.; Fontaine, M. N.; Rehel, K. V. Alteration of bacterial adhesion induced by the substrate stiffness. *Colloid Surface B* **2014**, *114*, 193-200.

(15) Gutekunst, S. B.; Grabosch, C.; Kovalev, A.; Gorb, S. N.; Selhuber-Unkel, C. Influence of the PDMS substrate stiffness on the adhesion of Acanthamoeba castellanii. *Beilstein J. Nanotechnol.* **2014**, *5*, 1393-1398.

(16) Zhang, R.; Ni, L.; Jin, Z.; Li, J.; Jin, F. Bacteria slingshot more on soft surfaces. *Nat. Commun.* **2014**, *5*, 5541.

(17) Saha, N.; Monge, C.; Dulong, V.; Picart, C.; Glinel, K. Influence of polyelectrolyte film stiffness on bacterial growth. *Biomacromolecules* **2013**, *14* (2), 520-528.

(18) Kolewe, K. W.; Kalasin, S.; Shave, M.; Schiffman, J. D.; Santore, M. M. Mechanical Properties and Concentrations of Poly(ethylene glycol) in Hydrogels and Brushes Direct the Surface Transport of Staphylococcus aureus. *ACS Appl Mater Interfaces* **2019**, *11* (1), 320-330.

(19) Valentin, J. D. P.; Qin, X.-H.; Fessele, C.; Straub, H.; van der Mei, H. C.; Buhmann, M. T.; Maniura-Weber, K.; Ren, Q. Substrate viscosity plays an important role in bacterial adhesion under fluid flow. *Journal of Colloid and Interface Science* **2019**, *552*, 247-257.

(20) Liu, M.; Sun, J.; Sun, Y.; Bock, C.; Chen, Q. Thickness-dependent mechanical properties of polydimethylsiloxane membranes. *J. Micromech. Microeng.* **2009**, *19* (3), 035028.

(21) Qi, M.; Song, Q.; Zhao, J.; Ma, C.; Zhang, G.; Gong, X. Three-Dimensional Bacterial Behavior near Dynamic Surfaces Formed by Degradable Polymers. *Langmuir* **2017**, *33* (45), 13098-13104.

(22) Avlyanov, J. K.; Josefowicz, J. Y.; MacDiarmid, A. G. Atomic force microscopy surface morphology studies of `in situ' deposited polyaniline thin films. *Synth. Met.* **1995**, *73* (3), 205-208.

(23) Radmacher, M.; Fritz, M.; Hansma, P. K. Imaging Soft Samples with the Atomic Force Microscope: Gelatin in Water and Propanol. *Biophys. J.* **1995**, *69* (1), 264-270.

(24) Dimitriadis, E. K.; Horkay, F.; Maresca, J.; Kachar, B.; Chadwick, R. S. Determination of Elastic Moduli of Thin Layers of Soft Material Using the Atomic Force Microscope. *Biophys. J.* **2002**, *82* (5), 2798-2810.

(25) Ong, Y. L.; Razatos, A.; Georgiou, G.; Sharma, M. M. Adhesion forces between E. coli bacteria and biomaterial surfaces. *Langmuir* **1999**, *15* (8), 2719-2725.

(26) Senden, T. J. Force microscopy and surface interactions. *Curr. Opin. Colloid In.* **2001**, *6*, 95-101.

(27) Lee, S. H.; Grier, D. G. Holographic microscopy of holographically trapped three-dimensional structures. *Opt. Express* **2007**, *15* (4), 1505-1512.

(28) Xu, W. B.; Jericho, M. H.; Meinertzhagen, I. A.; Kreuzer, H. J. Digital in-line holography for biological applications. *PNAS* **2001**, *98* (20), 11301-11305.

(29) Cheong, F. C.; Krishnatreya, B. J.; Grier, D. G. Strategies for three-dimensional particle tracking with holographic video microscopy. *Opt. Express* **2010**, *18* (13), 13563-13573.

(30) Eisenbach, M. *Encyclopedia of Life Sciences.* Nature Publishing Group: London, **2001**.

(31) Berg, H. C.; Brown, D. A. Chemotaxis in Escherichia coli analyzed by three-dimensional tracking. *Nature* **1974**, *19*, 55-78.

(32) Son, K.; Guasto, J. S.; Stocker, R. Bacteria can exploit a flagellar buckling instability to change direction. *Nat. Phys.* **2013**, *9* (8), 494-498.

(33) Xie, L.; Altindal, T.; Chattopadhyay, S.; Wu, X. L. Bacterial flagellum as a propeller and as a rudder for efficient chemotaxis. *PNAS* **2011**, *108* (6), 2246-2251.

(34) Kim, D.; Pertea, G.; Trapnell, C.; Pimentel, H.; Kelley, R.; Salzberg, S. L. TopHat2: accurate alignment of transcriptomes in the presence of insertions, deletions

and gene fusions. *Genome Biol.* **2013**, *14* (4), 13.

(35) Hopcroft, M. A.; Nix, W. D.; Kenny, T. W. What is the Young's Modulus of Silicon? *J. Microelectromech. S.* **2010**, *19* (2), 229-238.

(36) Vogel, R.; Pal, A. K.; Jambhrunkar, S.; Patel, P.; Thakur, S. S.; Reategui, E.; Parekh, H. S.; Saa, P.; Stassinopoulos, A.; Broom, M. F. High-Resolution Single Particle Zeta Potential Characterisation of Biological Nanoparticles using Tunable Resistive Pulse Sensing. *Sci. Rep.* **2017**, *7*, 13.

(37) McNeil, S. E. *Characterization of Nanoparticles Intended for Drug Delivery.* Springer: New York **2011**.

(38) Hoffman, M. D.; Zucker, L. I.; Brown, P. J. B.; Kysela, D. T.; Brun, Y. V.; Jacobson, S. C. Timescales and Frequencies of Reversible and Irreversible Adhesion Events of Single Bacterial Cells. *Anal. Chem.* **2015**, *87* (24), 12032-12039.

(39) Kang, H.; Shim, S.; Lee, S. J.; Yoon, J.; Ahn, K. H. Bacterial Translational Motion on the Electrode Surface under Anodic Electric Field. *Environ. Sci. Technol.* **2011**, *45* (13), 5769-5774.

(40) Niu, Q.; Wang, D. Probing the polymer anomalous dynamics at solid liquid interfaces at the single-molecule level. *Curr. Opin. Colloid In.* **2019**, *39*, 162–172.

(41) Berg, H. C. *E. coli in Motion.* Springer: New York, **2004**.

(42) Hernandez-Ortiz, J. P.; Stoltz, C. G.; Graham, M. D. Transport and collective

dynamics in suspensions of confined swimming particles. *Phys. Rev. Lett.* **2005**, *95* (20), 204501.

(43) Molaei, M.; Barry, M.; Stocker, R.; Sheng, J. Failed escape: solid surfaces prevent tumbling of Escherichia coli. *Phys. Rev. Lett.* **2014**, *113* (6), 068103.

(44) Valentini, M.; Filloux, A. Biofilms and Cyclic di-GMP (c-di-GMP) Signaling: Lessons from Pseudomonas aeruginosa and Other Bacteria. *J. Biol. Chem.* **2016**, *291* (24), 12547-12555.

(45) Galperin, M. Y. Diversity of structure and function of response regulator output domains. *Curr. Opin. Microbiol.* **2010**, *13* (2), 150-159.

(46) Sondermann, H.; Shikuma, N. J.; Yildiz, F. H. You've come a long way: c-di-GMP signaling. *Curr. Opin. Microbiol.* **2012**, *15* (2), 140-146.

(47) Hickman, J. W.; Harwood, C. S. Identification of FleQ from Pseudomonas aeruginosa as a c-di-GMP-responsive transcription factor. *Molecular Microbiology* **2008**, *69* (2), 376-389.

(48) Song, F. C.; Wang, H.; Sauer, K.; Ren, D. C. Cyclic-di-GMP and oprF Are Involved in the Response of Pseudomonas aeruginosa to Substrate Material Stiffness during Attachment on Polydimethylsiloxane (PDMS). *Front. Microbiol.* **2018**, *9*, 13.

(49) Poli, A.; Anzelmo, G.; Nicolaus, B. Bacterial Exopolysaccharides from Extreme Marine Habitats: Production, Characterization and Biological Activities. *Mar. Drugs*

2010, *8* (6), 1779-1802.

(50) Sutherland, I. W. Bacterial exopolysaccharides. *Adv. Microb. Physiol.* **1972**, *8*, 143-213.

Table of Contents